JOURNAL OF GEOPHYSICAL RESEARCH, VOL. 112, G01015, doi:10.1029/2006JG000280, 2007

Deriving daily carbon fluxes from hourly CO_2 mixing ratios measured on the WLEF tall tower: An upscaling methodology

Jing M. Chen,[1] Baozhang Chen,[1] and Pieter Tans[2]

Received 28 July 2006; revised 30 August 2006; accepted 4 October 2006; published 15 February 2007.

[1] The temporal variation of the CO_2 mixing ratio in the atmosphere at a given height results from several processes, including photosynthesis and respiration of the underlying ecosystems, the vertical mixing of the atmosphere near the surface and in the planetary boundary layer (PBL), and entrainment of the air above the PBL. Theoretically, if all atmospheric processes are modeled accurately, we can estimate the magnitude of ecosystem photosynthesis and respiration from the variations in the measured CO_2 mixing ratio. Through analyzing the CO_2 concentration measured at several heights (30 m, 122 m, and 396 m) on the Wisconsin tall tower, we demonstrate that it is possible to derive the daily carbon flux resulting from CO_2 uptake from hourly CO_2 mixing ratio data. At 30 m, the concentration-derived daily gross primary productivity (GPP) is well correlated with measured daily GPP derived from flux measurements ($r^2 = 0.70$), but the former was 20% larger than the latter. The correlation increased considerably for 10-day averages ($r^2 = 0.87$). As the variations at lower heights have larger diurnal CO_2 amplitudes, the concentration-derived GPP is more accurate at lower heights. The footprint distance of CO_2 concentration during the daytime under the influence of the mixed layer is estimated to be of the order of 10^3 km, or a footprint area of 10^3–10^4 km^2, which is much larger than that of CO_2 fluxes measured using eddy covariance methods (typically 1 km^2). The difference in these footprint areas may partly explain the differences between these two flux estimates at the Wisconsin tower. These differences also signify the importance of retrieving flux information from the mixing ratio as it provides a means to upscale from local sites to a region.

Citation: Chen, J. M., B. Chen, and P. Tans (2007), Deriving daily carbon fluxes from hourly CO_2 mixing ratios measured on the WLEF tall tower: An upscaling methodology, *J. Geophys. Res.*, *112*, G01015, doi:10.1029/2006JG000280.

1. Introduction

[2] In our efforts to understand the global greenhouse gas dynamics and to project the future climate, fast progress has been made in several areas of research in recent years. Carbon balance estimates at global and continental scales have been much improved through atmospheric inverse modeling [*Gurney et al.*, 2002; *Rodenbeck et al.*, 2003]. Many efforts have also been made to interpret and predict the role of terrestrial ecosystems in the global carbon balance [*Keeling et al.*, 1989; *Tans et al.*, 1990; *Denning et al.*, 1995; *Ciais et al.*, 1997; *Fung et al.*, 1997; *Wofsy and Harris*, 2002]. Ecosystem functioning and its effects on carbon balance have been much better understood than before through collecting and analyzing energy and CO_2 fluxes made at local sites using eddy covariance (EC) measurement techniques [*Baldocchi et al.*, 2001]. Direct measurements of the terrestrial carbon flux using these techniques are being made worldwide [*Baldocchi et al.*, 2001]. Currently there are over 250 EC tower stations worldwide in several research networks. However, EC measurements under Fluxnet programs represent only a very small fraction of the land area, typically about 1 km^2 for each site.

[3] These progresses have been achieved at the extreme ends of the spatial-scale spectrum, either large regions/continents or small vegetation stands. Because of the heterogeneity of the land surface and the nonlinearity inherent in ecophysiological processes in response to their driving forces, it is exceedingly difficult to upscale stand-level results to regions and the globe by extrapolation [*Levy et al.*, 1999]. Budgets of carbon at intermediate regional scales (10^2–10^6 km) can neither be scaled up from EC measurements [*Ehleringer and Field*, 1993; *Helliker et al.*, 2004] nor scaled down from the globe without considering the surface heterogeneity. Nevertheless, these intermediate scales are the necessary steps in increasing our confidence in regional and global carbon budgets. These scales also have direct relevance to natural resources management [*Newson and Calder*, 1989]. Hence there is a strong motivation to develop methods to use atmospheric observations to quantify and validate estimates of carbon balance at these intermediate scales [*Lin et al.*, 2004; *Bakwin et al.*, 2004]. These studies make use of measurements of the CO_2

[1] Department of Geography, University of Toronto, Toronto, Ontario, Canada.
[2] Climate Monitoring and Diagnostics Laboratory, NOAA, Boulder, Colorado, USA.

0148-0227/07/2006JG000280$09.00

mixing ratio in the planetary boundary layer (PBL), typically the midday minimum values, to estimate the net CO_2 exchange at daily or longer timescales on the basis of the PBL carbon budget. The PBL measurements naturally integrate the effects of the land ecosystems on the atmosphere at the landscape level and larger. This scale is ideal for our purpose of bridging the scale gaps in our carbon cycle estimation.

[4] The continuous CO_2 mixing ratio measured on tall towers contains information more than the net carbon exchange. The CO_2 diurnal variation pattern is influenced by the land surface metabolism, although it is also subject to fast and efficient mixing in the atmosphere at large scales. The focus of this present study is to extract ecosystem flux components, such as the gross primary productivity (GPP), from the diurnal variation pattern of the CO_2 mixing ratio, although it is notoriously difficult to estimate fluxes from concentrations [*Raupach*, 1995]. On the basis of our early work on simulating the hourly CO_2 mixing ratio through combining an ecosystem model with a vertical diffusion scheme [*Chen et al.*, 2004], we developed a methodology that allows the estimation of daily fluxes from hourly concentration measurements near Fraserdale, Canada [*Chen et al.*, 2006]. Concentration-derived flux information represents footprint areas of up to 10^5 km^2 [*Gloor et al.*, 2001; *Lin et al.*, 2004], which are several orders of magnitude larger than the direct flux measurements using EC techniques. This information is therefore much needed in our effort to upscale from site to region. It has been shown to be useful to investigate climate change impacts on boreal ecosystems at the landscape level [*Chen et al.*, 2006]. The purpose of this study is to use the concurrent CO_2 mixing ratio and flux measurements at several heights at the Wisconsin tall tower to explore the applicability and reliability of the methodology of deriving daily carbon fluxes from hourly CO_2 mixing ratio measurements. In particular, we seek to address the following questions: (1) How well does the concentration-derived GPP agree with flux-derived GPP? (2) How much does the concentration-derived GPP vary with height and what are the reasons? (3) What are the advantages and limitations of the concentration-derived GPP in comparison with EC flux measurements? As the concentration-derived GPP has a much larger footprint area than EC measurements, these questions bear significance in our ability to retrieve landscape-level carbon cycle information from atmospheric CO_2 measurements.

2. Materials and Methodology

2.1. Research Site and Measurements

[5] The WLEF television tower is located in the Chequamegon National Forest about 15 km east of Park Falls in northern Wisconsin, USA (45.94591°N, 90.27231°W). The region is in a heavily forested zone of low relief. A grassy clearing of 180 m radius surrounds the tower. The regional forest cover is documented in detail by *Mackay et al.* [2002] and *Davis et al.* [2003]. Briefly, 80% of the vegetation surrounding the tower comprised four major forest cover types: forested wetlands, upland aspen forests, upland northern hardwood forests, and upland pine forests. The rest of the area is mostly covered by grass (open meadow). The measured effective leaf area index (LAI) differed significantly among the five cover types and averaged 3.45, 3.57, 3.82, 3.99, and 1.14 for northern hardwoods, aspen, forested wetlands, upland conifers, and grass, respectively [*Burrows et al.*, 2002], while *Mackay et al.* [2002] concluded from measurements that "most of forests had LAI values in the range of 3.5–4". The average LAI for the 3 × 2 km area centered on the flux tower of 3.51 ± 0.89 (with a minimum of 0 and a maximum of 6.35), as measured by *Burrows et al.* [2002], is taken as the mean LAI value for the area in our model. As the measured LAI values are effective LAI assuming the random leaf spatial distribution, we take it as the true LAI assuming that woody area is offset by the clumping of the foliage [*Chen et al.*, 1997]. Vegetation foliage clumping significantly alters its radiation environment and therefore affects water and heat as well as carbon cycle. In our model, the clumping index (Ω) is used for accurate separation of sunlit and shaded leaves in the canopy, and we set $\Omega = 0.75$ for this area.

[6] The maximum canopy height in the region is about 25 m. Wetlands tend to have substantially lower canopies as do young aspen stands. Soils are sandy loam and are mostly glacial outwash deposits. The site is at the northern edge of the Mississippi River Basin. Distributions of soil properties correspond to the landform, forest ecosystem dynamics and management activities, i.e., as documented by *Burrows et al.* [2002]: red pine (*Pinus resinosa* Ait) and jack pine (*Pinus banksiana* Lamb) dominate areas of excessively drained sandy soils derived from glacial outwash; northern hardwood forests, comprising sugar maple (*Acer saccharum* Marsh.), red maple (Acer rubrum L.), green ash (*Fraxinus americana* Marsh.), yellow birch (*Betula alleghaniensis* Britton), and basswood (*Tilia americana* L.), occur on the finer-textured soils in moraines and drumlins. Soils of intermediate characteristics support a wide variety of broadleaf deciduous tree species, such as paper birch (*Betula papyrifera* Marsh), quaking aspen (*Populus tremuloides* Michx), bigtooth aspen (*Populus grandidentata* Michx), red maple, and red and white pine (*Pinus strobus* L.). Soil properties data, used as our model inputs, are averaged values for the 3 × 2 km area centered on the flux tower (similar to LAI calculation) from GIS maps available at http://www.ncrs.fs.fed.us/gla/maps.htm. Combining our knowledge on forest soil characteristics with the parent materials of soil origination (that is mostly glacial outwash deposits), the four-layer profile of soil texture classes are approximated as loam (0–0.2 m), sandy loam (0.2–0.45 m), clay silt (0.45–0.95 m), and silty clay (0.95–2.45 m), respectively.

[7] The site, instrumentation, and flux calculation methodology have been described by *Bakwin et al.* [1998], *Berger et al.* [2001], and *Davis et al.* [2003]. Instruments were mounted on a 447 m television transmitter tower. Carbon, water and sensible heat fluxes were measured at three heights at 30, 122, and 396 m above the ground using eddy covariance methods, and mean CO_2 mixing ratios were sampled in 2-min intervals at six levels at 11, 30, 76, 122, 244, and 396 m.

2.2. Modeling Methodology

2.2.1. Models for Ecosystem Fluxes and Atmospheric Diffusion

[8] The carbon cycle involving soil, vegetation and atmosphere is simulated using an integrated model system

Table 1. Comparison Between Modeled and Observed Monthly Mean Daily Maxima of Convective PBL z_{max} in the Vicinity of the WLEF Tall Tower[a]

	Month											
	1	2	3	4	5	6	7	8	9	10	11	12
Obs, 1998	na	na	1490	1720	2030	1940	1930	1820	1510	1340	na	na
Mod, 2001	928	1383	1528	1819	1990	1980	1872	1722	1469	1274	1103	953
Mod SD	194	374	287	513	364	425	413	249	195	277	203	198

[a]Obs represents observed monthly mean z_{max} in 1998 by *Yi et al.* [2001]; Mod represents simulated monthly mean z_{max} in this study for 2001, and SD is the standard deviation of simulated monthly mean z_{max}.

consisting of two components: the Vertical Diffusion Scheme (VDS) [*Chen et al.*, 2004] and the Boreal Ecosystem Productivity Simulator (BEPS) [*Chen et al.*, 1999; *Liu et al.*, 1999, 2002]. BEPS used in this study is a new version that includes a land surface scheme: Ecosystem-Atmosphere Simulation Scheme (EASS) [*Chen et al.*, 2006]. This BEPS version simulates, at hourly time steps, ecosystem processes including soil water balance, photosynthesis, autotrophic and heterotrophic respiration, and radiation and energy balances of the canopy and soil surface. The total soil carbon is determined through a spinup procedure similar to that of *Chen et al.* [2003a]. In BEPS, photosynthesis is calculated on the basis of Farquhar's leaf-level model [*Farquhar et al.*, 1980] with an upscaling procedure through sunlit and shaded leaf stratification. In this stratification, the importance of canopy structure is considered using a foliage clumping index [*Chen et al.*, 2003b]. This hourly model has been intensively validated using eddy covariance flux data for CO_2 [*Ju et al.*, 2006] and water [*Chen et al.*, 2006] at Canadian sites.

[9] The VDS model simulates CO_2 diffusion within the PBL under both stable and unstable conditions [*Chen et al.*, 2005]. It is a one-dimensional bottom-up and top-down vertical mixing model similar to those of *Wyngaard and Brost* [1984] and *Moeng and Wyngaard* [1989]. In VDS, the mixed layer is stratified into 50 m layers and constant bottom-up and top-down mixing coefficients are used throughout the mixed layer at a given time [*Zhang and Anthes*, 1982]. This model setup allows the CO_2 concentration at each layer to vary with time according the vertical concentration gradient and the mixing coefficients at each time step (30 s) without using the quasi-steady state assumption for the vertical gradient [*Moeng and Wyngaard*, 1989]. VDS is updated since *Chen et al.* [2004] for the purpose of this study. For the convenience of comparison with the tower measurements, the lower surface layers in this model are set at the CO_2 measurement heights of 30, 76, 122, 172, 208, 244, 294, 344 and 396 and 450 m. The levels above 450 m are separated in regular intervals of 50 m in the model domain (2550 m). The model is improved through the use of short time steps (30 s rather than 60 s in work of *Chen et al.* [2004]) and modified schemes to treat the stable/nocturnal and the free-convection PBL structures. The atmospheric stability determines the selection of a stable or free convection scheme. The criteria for the selection are the sign and magnitude of the bulk Richardson number R_b in the surface layer and the magnitude of $|z_h/L|$, where z_h denotes the height of the mixed layer and L is the Monin-Obukhov length. R_b is calculated using equation (5.6.3) from *Stull* [1993]. For estimating the entrainment of CO_2 at the top of the mixed layer, the Globalview CO_2 matrix data in 41 latitudinal bands based on weekly flask samples in the marine boundary layer (MBL) for the year 2001 [*National Oceanic and Atmospheric Administration*, 2004] are linearly interpolated to represent CO_2 concentration in the free troposphere (FT) at the WELF tower as the top boundary condition of the PBL. The influences of clouds and large-scale vertical mixing associated with frontal systems on the entrainment have not been considered, and the subsidence affecting the mixed layer development is not explicitly modeled. Within this simple one-dimensional model, systematic errors in entrainment and mixed layer development are minimized by ensuring that the mean monthly mixed layer height is estimated accurately in comparison with available measurements (see Table 1, discussed in section 2.2.2).

[10] BEPS and VDS are linked through two prognostic variables: land surface sensible heat flux (H) affecting the mixed layer development, and net ecosystem carbon flux (NEE) giving rise to the vertical CO_2 transfer. Modeled hourly H results are validated against eddy covariance data at the tower, with $r^2 = 0.60$ and RMSE = 60.5 W m^{-2} s^{-1} (n = 7152). A comprehensive validation of NEE is shown in section 3.

2.2.2. Methods for Isolating Photosynthesis Signals

[11] As the air CO_2 mixing ratio at a given height is determined by both the surface metabolism and atmospheric mixing processes, it would be possible to isolate the signals for the metabolism if the atmospheric diffusion is accurately modeled. However, to ensure a reasonable accuracy in modeling the diffusion processes, we first need to simulate the variability of the CO_2 mixing ratio to a satisfactory accuracy. This requires that both the ecosystem metabolism and atmospheric diffusion are well simulated. The atmospheric diffusion here involves nighttime stable boundary diffusion and daytime mixed layer development and entrainment. The ecosystem metabolism (photosynthesis and respiration) simulated for the purpose of matching with the observed CO_2 mixing ratio under a given regime of the atmospheric turbulence is considered to be the first-order estimate and can be much improved using a new methodology employed here.

[12] The methodology is illustrated in Figure 1 showing a 1-day example, where the simulated hourly CO_2 concentration at 30 m was compared with the observation on the WELF tower. It must be realized that to mimic the diurnal variation in the CO_2 mixing ratio, both diffusion and metabolism have to be simulated with reasonable accuracies, although it is still possible that an underesti-

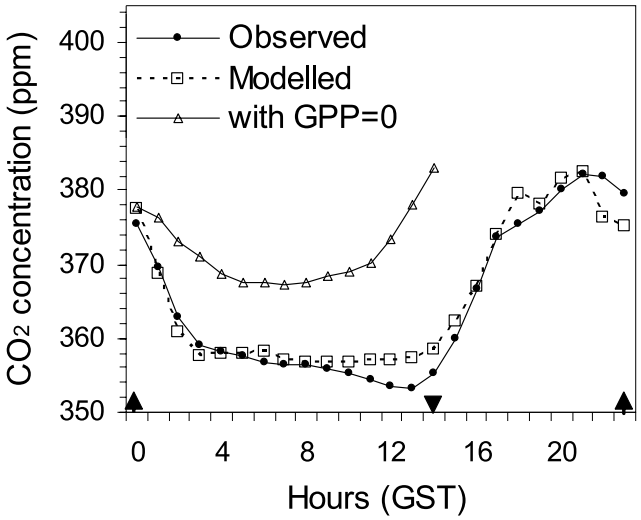

Figure 1. An example of measured and modeled CO_2 mixing ratio at 30 m above the ground, 26 July 2001 (GST). GST is 6 hours ahead of the local standard time. Also shown is the modeled CO_2 mixing ratio with $GPP = 0$ at daytime. Triangles indicate the times of sunrise and sunset.

mation of photosynthesis is offset by an underestimation of the PBL height at daytime or an overestimation of turbulent mixing in the surface layer. However, this mutual error dependence can be minimized when PBL model results are validated against existing data, and both wind and temperature gradient measurements are used in the estimation of atmospheric stability in the surface layer. The monthly mean diurnal evolution patterns of mixed layer z_i for 2001 simulated at hourly time steps are similar to observations made at the same site for 1998 [*Yi et al.*, 2001]. The simulated monthly mean daily maximum of PBL (z_{max}) for 2001 and those observed for 1998 are compared in Table 1. Both the simulated and observed seasonal values of z_{max} occurred in May, corresponding to the maximum sensible heat flux prior to full leaf-out, not maximum net radiation which occurred in June and July. The surface energy balance from July to August was mostly partitioned by a large latent heat flux due to evapotranspiration. April was also characterized by deep (even about 100 m deeper than measured in 1998, Table 1), well-developed mixed layers due to generally large sensible heat fluxes. Modeled z_{max} in August and in September for 2001 were lager than that measured in 1998 (Table 1), and this discrepancy may be caused by model errors but also possibly induced by annual variations in precipitation and hence in the partitioning of sensible heat and latent heat fluxes. The overall differences in monthly mean z_{max} between modeled for 2001 and measured for 1998 are within 100 m.

[13] These close agreements between the model and observation indicate that the PBL dynamics and diffusion processes are satisfactorily simulated for the purpose of estimating the CO_2 profile within the PBL. We then turn off the gross primary productivity in the model, i.e., setting $GPP = 0$ without changing *ER*, and simulate the evolution of the CO_2 mixing ratio with time from sunrise to sunset. The curve with $GPP = 0$ gradually departs from the observed curve, and stays at a certain level during the well mixed hours because of the large capacity of the mixed layer and then increases in the late afternoon when respiration exceeds photosynthesis. The difference between the curve with $GPP = 0$ and the observed curve is then entirely due to *GPP*, or the accumulated hourly difference is proportional to the daily total *GPP* (see section 3), if other processes (diffusion and respiration) are simulated accurately. In this way, the signal due to daytime photosynthesis is extracted from the CO_2 record. The main advantage of this methodology over the first-order estimation, i.e., tuning *GPP* to match the CO_2 record, is that it involves no assumption of horizontal homogeneity or directional variability because the *GPP* signal extracted this way is the true *GPP* in the footprint area, however spatially variable and wherever may it be.

[14] Physically, the hourly difference in CO_2 (ΔC_i, in ppm or μmol mol^{-1}) between the measured and simulated (with $GPP = 0$) cases is the reduction of CO_2 by *GPP* per unit air volume in the mixed layer. Assuming that this reduction is uniform in the mixed layer, the simulated mixed layer height z_i can then be used to estimate the *GPP* per unit surface area as $\Delta C_i\, z_i\, \rho_{air}$ (μmol m^{-2}), where ρ_{air} is the dry air density in mol m^{-3}. As the air moves across the landscape, this effect of *GPP* on air CO_2 gradually accumulates. For hour i after sunrise, the total accumulated effect is $\Delta C_i\, z_i\, \rho_{air}$, and *GPP* in this hour is $(\Delta C_i\, z_i - \Delta C_{i\text{-}1}\, z_{i\text{-}1})\rho_{air}$. The daily total GPP is then equals

$$\mathrm{GPP} = \sum_{i=SR+1}^{SS} (\Delta C_i z_i - \Delta C_{i-1} z_{i-1})\rho_{air} = \rho_{air} \Delta C_{ss} z_{ss}, \qquad (1)$$

where *SR* is the sunrise hour, *SS* is the sunset hour, and C_{ss} and z_{ss} are the CO_2 mixing ratio and mixed layer height at sunset, respectively. At the sunrise, ΔC_{SR} is zero. The accumulation of this photosynthesis effect starts at sunrise and moves with the air from sunrise to sunset, and the tower CO_2 measurements therefore integrate the influence of the land surface over the daily air travel length upwind of the tower. In deriving equation (1), the following assumptions are made: (1) the mixed layer is well mixed so that the difference in CO_2, i.e., ΔC_i, before and after turning off *GPP* does not vary with height significantly, (2) no advection effects (advection of a different airmass would affect the measured CO_2 but not the modeled CO_2 with $GPP = 0$, and therefore its effect is included in the concentration-derived *GPP*), and (3) other CO_2 sources, such as biomass burning and fossil fuel combustion, are negligible or does not change with time. Since this *GPP* derivation methodology is based on the diurnal variation pattern, the effects of other CO_2 sources are removed when they increase the CO_2 concentration uniformly with time. At nighttime the atmosphere is highly stratified, and the similar assumption of uniform vertical mixing within the PBL is no longer valid. This methodology is therefore not used to extract nighttime *ER*.

[15] The complete procedure of daily *GPP* estimation from hourly CO_2 concentration measurements is outlined in Figure 2. The BEPS model produces carbon and sensible heat fluxes at hourly time steps according to hourly mete-

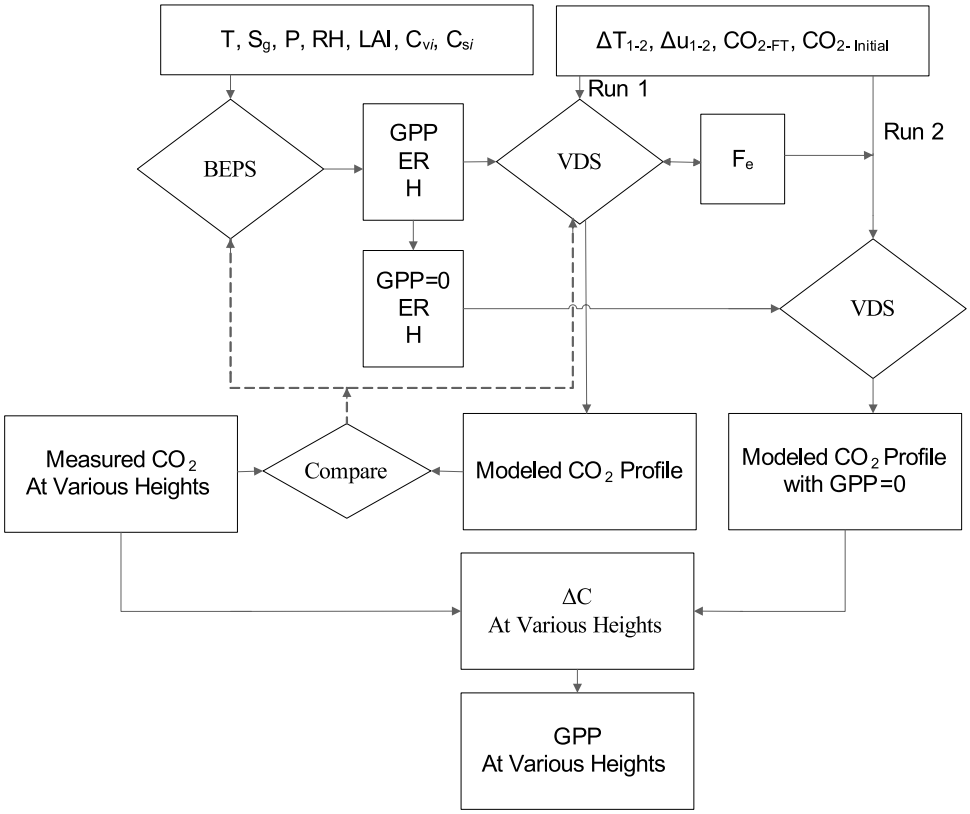

Figure 2. Procedures for deriving gross primary productivity (*GPP*) from tall tower CO_2 concentration measurements using models of the Boreal Ecosystem Productivity Simulator (BEPS) and the Vertical Diffusion Scheme (VDS). These procedures are repeated hourly from sunrise to sunset in order to obtain the daily GPP values. The mean inputs to BEPS are air temperature T, global solar radiation S_g, precipitation P, relative humidity RH, leaf area index LAI, vegetation carbon pools (leaf, stem, root) C_{vi}, and total soil carbon pools in four layers C_{si}. The mean inputs to VDS are vertical temperature gradients ΔT_{1-2}, wind speed gradients Δu_{1-2}, CO_2 concentration in the free troposphere $CO_{2\text{-FT}}$, and the initial daily CO_2 at midnight in the residue layer $CO_{2\text{-initial}}$ (above the stable PBL and below the mixed layer height of the previous day). The modeled fluxes are the ecosystem respiration ER ($NEP = GPP\text{-}ER$), sensible heat flux H, and the entrainment flux F_e.

orological data and estimated vegetation and soil carbon pools through a spinup procedure [*Chen et al.*, 2003a]. In the first VDS run, the hourly CO_2 profile within the mixed layer and the CO_2 entrainment are computed on the basis of the sensible heat flux modeled by BEPS, temperature and wind speed gradients measured on the tower, the CO_2 concentration in the free troposphere, and the initial CO_2 profile below the free troposphere (updated at each midnight using the measured minimum value in the previous day). The differences between the modeled and measured CO_2 mixing ratios at various heights at different times are first used to fine tune both BEPS and VDS. The tunable parameters include the maximum stomatal conductance, the maximum carboxilation rate, and the soil carbon respiration coefficients at the base temperature (10°C) in BEPS [*Chen et al.*, 1999] and the surface roughness in VDS. In the second VDS run, the *GPP* produced by BEPS is set to zero while keeping all other hourly fluxes unchanged from the previous run, including respiration and entrainment. In this way a new modeled CO_2 profile is produced, and from the differences between measured and modeled CO_2 mixing ratios at the various heights, hourly and then daily *GPP* values at these heights are derived.

2.3. Methods for Data Gap Filling

2.3.1. Filling Gaps in Flux Data

[16] The WLEF tower was particularly challenging as a measurement program because of the logistics of servicing instruments on the tower, and frequent harsh conditions especially at the upper measurement levels [*Davis et al.*, 2003]. Three flux levels provided a greater temporal coverage than would otherwise be possible, but gaps with no valid flux data at any level still existed. In 2001, about three fourths of hours had EC flux measurements from at least one level. Available data at the lowest level (30 m) were much more than those at the other two levels. There were around two thirds of hours in 2001 having valid flux measurements after filtering the nighttime flux data with a threshold u_* value of 0.2 m s^{-1}. In this study, small data gaps of one to two hours are filled by linear interpolation. Gaps of durations $\geq$3 hours (up to 2 weeks) are filled using BEPS model results.

[17] *NEE* can be taken as the sum of the measured turbulent flux and the rate of change in C storage in the air column below the measurement height, following the typical assumption that the horizontal advection term is negligible [*Davis et al.*, 2003; *Chen et al.*, 2004], i.e.,

$$NEE_0 = F_{Cst} + F_{Ctb}, \tag{2}$$

where the subscript 0 denotes the flux at the canopy height and emphasizes that this is an approximation that depends on the transport being one-dimensional [*Yi et al.*, 2000]. The first term F_{Cst} on the right-hand side of (2) is the CO_2 storage flux, which is calculated from the CO_2 profiles measured on the tower. The second term is the turbulent flux F_{Ctb}, which is a direct EC flux measurement.

[18] Since turbulent fluxes are measured at three different heights on the WLEF tower it is possible to derive three estimates of NEE_0 when all instruments are operational. As discussed by *Davis et al.* [2003], if the surface flux is homogeneous within the footprint of all three flux measurements and advection of CO_2 is negligible (i.e., $NEE = NEE_0$), then NEE_0 will be identical for all three measured levels. All the three flux levels provide about three fourths of temporal coverage in 2001, that is, about one fourth gaps with no valid flux data still exist. In practice, the multiple levels can be used interchangeably to compute NEE_0 when data are missing at any one level [*Davis et al.*, 2003]. An optimal algorithm for computing *NEE* of CO_2 developed by *Davis et al.* [2003] is also used in this study. If data from all flux levels are present, we switch among levels according to stability, and use the sensible heat flux (H) as our indicator of stability. More details were documented by *Davis et al.* [2003].

[19] In the absence of the direct carbon release during disturbance, NEE_0 of CO_2 (exchange between terrestrial ecosystems and the atmosphere) is the result of carbon uptake during photosynthesis (*GPP*) and carbon loss due to respiration (total ecosystem respiration, *ER*),

$$NEE_0 = ER - GPP. \tag{3}$$

[20] In usual convention, the positive NEE_0 is a flux of CO_2 into the atmosphere, and both *ER* and *GPP* are positive. *ER* is a composite flux, involving respiration by foliage, stem, and roots (autotrophic respiration) and respiration by soil organisms (heterotrophic respiration). However, partitioning NEE_0 into *GPP* and *ER* components is a challenge because NEE_0 is typically an order of magnitude smaller than these two nearly offsetting terms.

[21] The values of NEE_0 during nighttime are taken as nighttime ecosystem respiration (*ER*). A simple approach is used to estimate daytime *ER* on the basis of regressions of nocturnal *ER* against soil temperature [e.g., *Janssens et al.*, 2001; *Valentini et al.*, 2000]. *GPP* can be obtained from equation (3) once daytime *ER* is estimated. Simulations of NEE_0 and its components *GPP* and *ER* with BEPS are used for filling data gaps.

2.3.2. Filling Gaps in the Temperature Profile

[22] As the CO_2 mixing ratio was measured more accurately, at more heights and more continuously than the air temperature on the WLEF tower, CO_2 gradient data are used to supplement the temperature gradient data in the estimation of atmospheric stability. At the height of 122 m, the measured temperature was consistently incompatible with those at other adjacent heights, and the temperature gradients immediately above and below this height were estimated from CO_2 gradients. On the basis of the similarity theory in turbulence transfer [*Stull*, 1993], the following equation was derived to replace or estimate the potential temperature gradient with the concentration gradient:

$$\theta_2 - \theta_1 = \frac{\rho_c H}{\rho C_p F_c}(C_2 - C_1), \tag{4}$$

where θ_1 and θ_2 are the potential temperatures at heights 1 and 2 (in °K), C_1 and C_2 are the CO_2 mixing ratios at the corresponding heights (dimensionless), H is the sensible heat flux in W m^{-2}, F_c is the CO_2 flux (NEE_0) in g C m^{-2} s^{-1}, ρ is the air density in g m^{-3}, C_p is the specific heat of the air in J g^{-1} °K^{-1}, and ρ_c is the density of CO_2 in the air in g m^{-3}. Both H and F_c were mostly measured at the 30 m height on the tower. When they are missing, their values are filled using BEPS model results.

3. Results

3.1. Atmospheric Diffusion and Ecosystem Modeling

[23] The critical step in our methodology of extracting the photosynthesis signal from the CO_2 record is to ensure that the atmospheric diffusion is simulated with a reasonable accuracy. Figure 3 provides examples of the simulated CO_2 mixing ratio in comparison with observed values at three heights on 5 consecutive days in July 2001. The simulated curves at the three heights generally follow the observed curves closely, even though the simulation is made with a simple one-dimensional model. The simulated curves are generally smoother than the observed values because of the assumption of horizontal homogeneity used in the 1-D model. At nighttimes, the observation sometimes shows a rapid buildup of CO_2 near the surface (30 m) followed by sharp drops when the stable boundary layer collapses briefly under gravity waves [*Mahrt et al.*, 1998]. These features are not yet captured in the 1-D model. However, the effects of these brief events on the net CO_2 exchange would diminish at daily and longer timescales. There are also synoptic events (frontal systems) causing abrupt changes in CO_2 concentration, and simulated results of the 1-D model have the largest departure from measurements under these circumstances.

[24] Similar simulation results are obtained for all days in 2001, and the results are summarized in Table 2 in terms of regression statistics between modeled and observed CO_2 concentrations at different heights. The r^2 value increases and the root mean square error (RMSE) decreases as the modeled hourly values are averaged for daily and 10-day periods, suggesting that the 1-D model can capture the underlying ecosystem variability for regional carbon balance estimation. As an extension from Table 2, Figure 4 shows the monthly averaged diurnal variations in CO_2 from January to December in 2001. For monthly averages, the simulated results are better compared with the observation at all three heights than the daily cases shown in Figure 3, because synoptic effects and other abrupt changes are

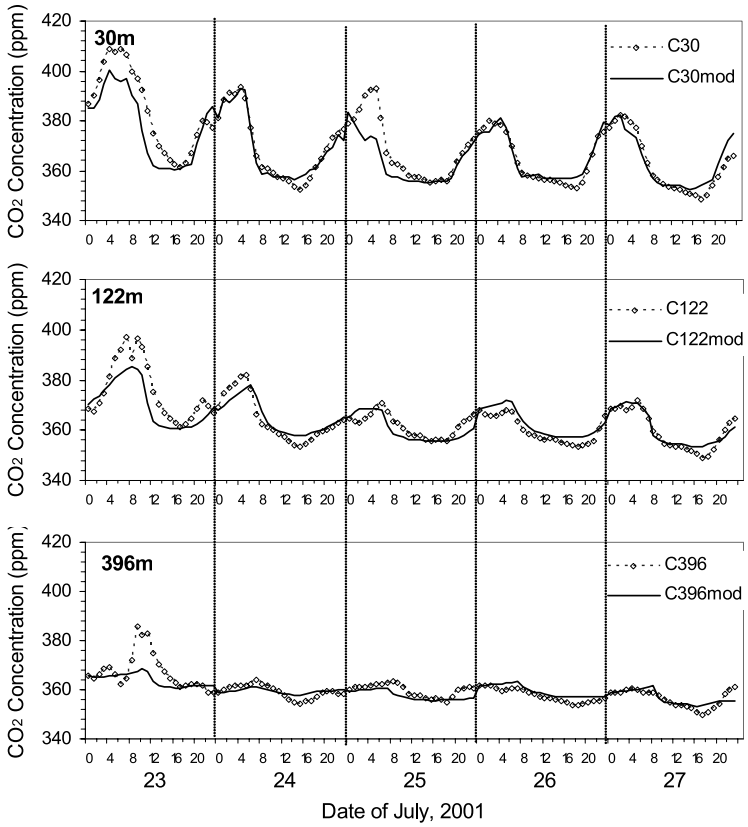

Figure 3. Comparison of measured (symbols) and modeled (solid line) CO_2 mixing ratios for 5 days in July 2001 at three heights (30 m, 122 m, and 396 m). Note that the diurnal amplitude decreases greatly with height.

smoothed out to a large extent. There are discontinuities at the monthly borders because of the realistic changes at monthly steps. The diurnal amplitude decreases greatly with height, especially in spring and summer months, because the nighttime stable boundary layer was generally very shallow (less than 200 m) [*Yi et al.*, 2004] and the increase in CO_2 is strongest at the lowest height at nighttime. Also shown in Figure 4 are curves of CO_2 concentration simulated with $GPP = 0$. These curves are analyzed together with Figure 8 in section 3.2. In order to show details of the diurnal variations of the various curves, the results in July are amplified in Figure 5, also to be discussed with Figure 8 in section 3.2.

[25] To ensure that atmospheric diffusion is simulated with an acceptable accuracy for our purpose of using a CO_2 record for deriving ecosystem information, we should also have the first-order estimate of the CO_2 flux to and from the underlying the surface, although we realize that both the soil and the vegetation cover are heterogeneous and cannot be well represented within our 1-D model using vegetation and soil data in the vicinity of the tower (section 2.1). Figure 6 shows the hourly CO_2 flux simulated with BEPS together with the canopy-level flux derived from those measured at the three heights (excluding gap-filled data). As BEPS simulates fluxes at the canopy level, the measured fluxes at 30 m, 122 m and 396 m need to be extrapolated to the canopy level in consideration of the atmospheric carbon storage change below a given measurement height. Both measured fluxes and storage corrections at the three heights were provided in the WLEF database. All three levels of measured fluxes were converted to the canopy level in this way to form a complete hourly flux series for the year. Again, the modeled fluxes do not show abrupt variations as shown in measured fluxes, suggesting the complex air mass movement from different portions of the landscape is not well captured in the 1-D model.

Table 2. Relationship Between Modeled and Observed CO_2 Concentrations at Different Heights From Hourly to 10-Day Mean Values[a]

	r^2			RMSE, μmol mol^{-1}			Sample Size (n)		
	Hourly	Daily	10-Day	Hourly	Daily	10-Day	Hourly	Daily	10-Day
30 m	0.69	0.70	0.88	5.2	3.63	1.82	8069	299	36
122 m	0.79	0.88	0.98	3.79	2.84	1.15	8069	299	36
396 m	0.83	0.91	0.97	3.33	2.6	1.92	8069	299	36

[a]Here r^2 is the linear regression coefficient; RMSE is the root mean square error, $= \sqrt{\frac{1}{n}\sum_{i=1}^{n}[C_{\mathrm{mod}}(i) - C_{obs}(i)]^2}$.

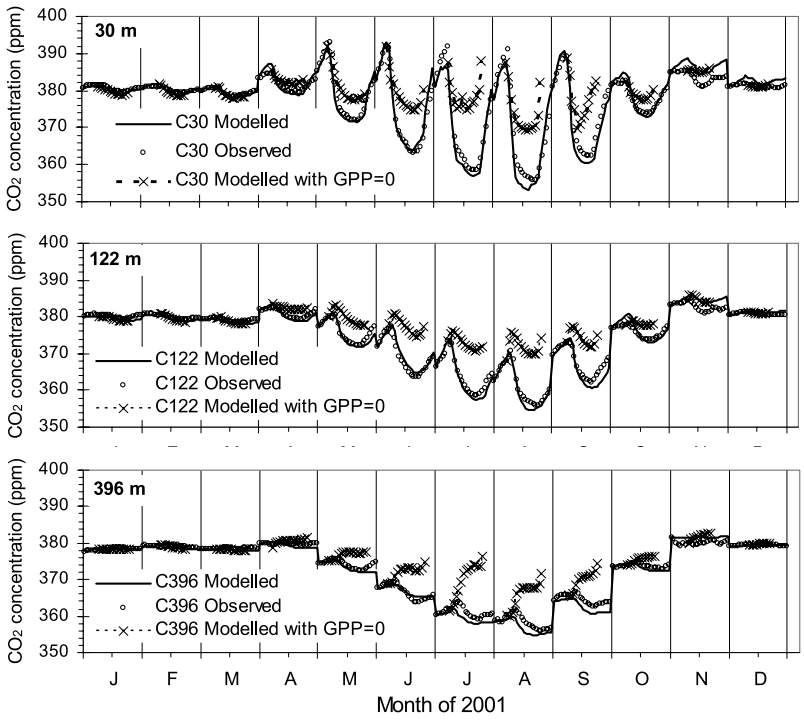

Figure 4. Monthly averaged diurnal variations of modeled (symbols) and observed (solid line) CO_2 mixing ratios at three heights in 2001. The differences between the modeled ratio with $GPP = 0$ and the observations from sunrise to sunset is the reduction of CO_2 caused by the surface photosynthesis.

[26] The performance of BEPS for simulating the diurnal variation in the CO_2 flux for all days in the year is summarized in Figure 7, in comparison with the measured fluxes extrapolated to the canopy level. In this comparison, the gap-filled flux data are excluded. The results are shown as monthly averaged diurnal variations in the flux. The model captured the upward flux due to nighttime respiration and the downward flux due to photosynthesis less respiration, with both the magnitude and phase in close agreement with measurements in all months. This, in combination with the CO_2 concentration simulation shown in Figure 4, gives confidence in the simulation of vertical atmospheric diffusion by VDS.

3.2. Extracting Flux Signals From the CO_2 Record

[27] Although BEPS simulated, with reasonable accuracy, the measured C flux at the canopy height (as shown in Figures 6 and 7), the results can only be considered as the first approximation of the ecosystem flux as the assumption of the horizontal homogeneity is made in the 1-D model. The atmospheric CO_2 measurements as affected by the horizontal heterogeneity can, in fact, be used to remove this assumption and improve the flux estimation. This is the focus of this study.

[28] After we gained confidence in modeling the atmospheric diffusion and ecosystem metabolism, the methodology illustrated in Figure 2 is applied to the entire record of CO_2 in 2001. Daily *GPP* values are computed for the whole year from the hourly CO_2 concentration measurements based on equation (1). Figure 8 shows comparisons of these concentration-derived *GPP* values at the three heights with those derived from flux measurements adjusted to the canopy height (after the storage correction), in daily and 10-day averaged values, separately. All daily values are highly variable (modeled daily results at 122 m and 396 m are not shown but have similar variability), and the seasonal variation patterns at these three heights are clearly shown in 10-day averages (Figure 8b). These patterns are similar to that of measurements, but they differ significantly in magnitude. As shown in Figure 5, as the height increases, the timing of the occurrence of the CO_2 decrease from the nighttime maximum is delayed, and the magnitude of the decrease is substantially subdued. As most CO_2 released from the ecosystem at nighttime accumulates in the lower atmosphere close to the ground, photosynthesis in the morning, before the mixed layer was fully developed, first consumed this nighttime accumulated CO_2, and the decrease in CO_2 at heights above the nighttime stable boundary layer (such as 396 m) only occurred when the accumulated amount of photosynthesis uptake exceeded the nighttime respiration release. In July, the delay of the surface photosynthesis effect on the CO_2 concentration was about 1–2 hours from about 7 am to 9 am between 30 m and 396 m (Figure 5). At the intermediate heights within the nighttime stable boundary layer, the decrease was also related to the strength of vertical mixing allowing the air aloft with low CO_2 concentration to mix with the lower layers. It is therefore expected that in the early morning the effect of photosynthesis uptake at the surface on the air CO_2 concentration decreased rapidly with height, and conversely, the concentration-derived hourly *GPP*, which was determined by the hourly additional reduction of CO_2, decreased with height. As the mixed layer further developed

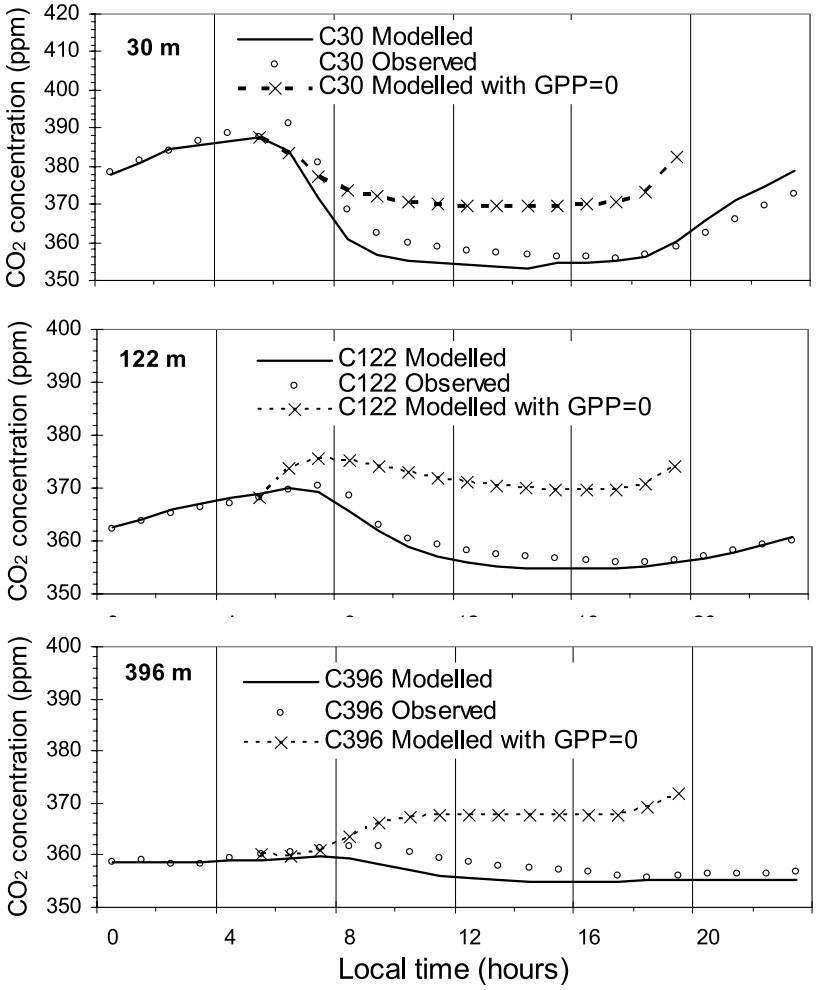

Figure 5. Monthly averaged diurnal variations of modeled (symbols) and observed (solid line) CO_2 mixing ratios at three heights in July 2001. This is an enlarged portion of Figure 4.

near noon and in the afternoon, the measured CO_2 concentration displayed little change with height and so did those modeled with $GPP = 0$ (Figures 4 and 5). In Figures 4 and 5, the differences between the curves with $GPP = 0$ and the measured curves are the accumulated amounts of reduction of CO_2 due to the gross photosynthesis. As a result of the near uniform vertical distributions of both measured and modeled CO_2 concentrations in the afternoon, the daily *GPP* value derived on the basis of the accumulated difference between the modeled and measured CO_2 at the sunset differed much less with height than the hourly values in the early morning, supporting the methodology of deriving daily *GPP* values rather than hourly values in order to take the advantage of the well mixed boundary layer in the late afternoon.

[29] For quantitative assessment of the variation of concentration-derived *GPP* with height, the results in Figure 8 are shown differently in Figure 9, where the concentration-derived *GPP* at the three heights are correlated with the flux-derived *GPP* at the canopy height. The correlation between the daily values is highest at the lowest level (at 30 m, $r^2 = 0.70$), but is much improved between 10-day averaged values (at 30 m, $r^2 = 0.87$). The large improvement in the correlation from daily to 10-day values shows the limitation of the 1-D model in estimating carbon fluxes at short timescales. As the air flow came from different directions with different underlying surfaces, including forests of various types and densities, cropland, grassland, and lakes [*Davis et al.*, 2003], large day-to-day variations were expected even though the meteorological conditions remained the same, but this variability cannot be captured by the 1-D model without spatially explicit land surface input. In addition to this variability, meteorological conditions associated with synoptic events could have changed frequently, and the strong vertical mixing associated frontal passages may violate some model assumptions for the mixed layer dynamics [*Yi et al.*, 2004; *Chan et al.*, 2004]. However, it is encouraging to see that monthly averaged diurnal variations of CO_2 mixing ratio at various heights are well simulated using the 1-D model (Figure 4) and that the concentration-derived 10-day averaged *GPP* values are highly correlated with flux-derived *GPP* (Figure 9). The 10-day averaging operation effectively reduces the influence of the spatial variability of the underlying surface on the flux estimation and greatly suppressed the effect of synoptic variability. As the derivation of *GPP* from CO_2 concentration makes no assumption of the spatial homoge-

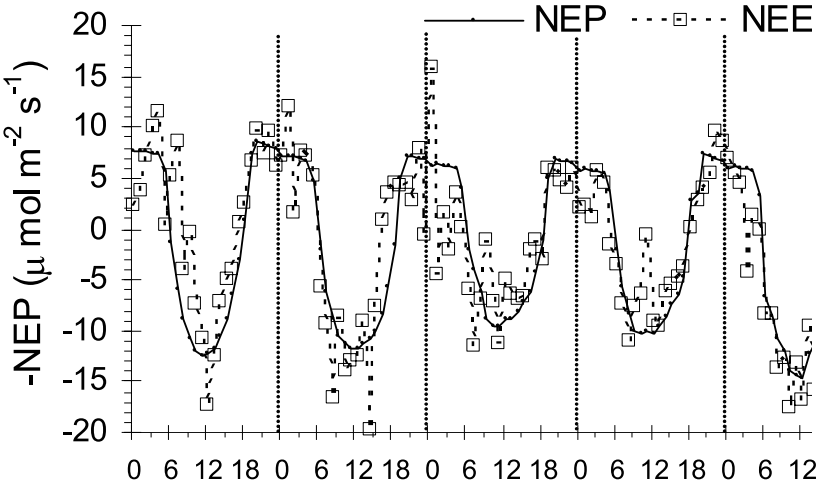

Figure 6. *NEP* calculated by BEPS compared with NEE_0 measured by an eddy covariance system at 30 m, 122 m, and 396 m and extrapolated to the canopy height after considering the carbon storage term for 23–27 July 2001.

neity, its value should represent the upwind area of the tower in the direction of wind on a given day. The large scatters in the 1:1 plots of the daily values in Figure 9 may mostly reflect the fact the footprint areas of flux and concentration measurements are different (further discussed below), and therefore should not be entirely taken as model errors, although these scatters could also be caused by errors in mixed layer simulations due to clouds and variable subsidence. The largest concern in using this derivation methodology is the extent to which the 1-D mixed layer dynamics are in error owing to variable synoptic conditions. Further research can be taken to quantify such errors for several major weather patterns to improve daily *GPP* estimates.

4. Discussion

[30] Two issues become apparent in the results shown in Figures 8 and 9: (1) concentration-derived GPP decreases with height, and (2) it differs systematically from the flux-derived GPP. These two issues are central to the uniqueness of the information that can be retrieved from the atmospheric CO_2 mixing ratio and are therefore further discussed below.

[31] The slope of the regressions in Figure 9 decreases significantly with height, from 1.20 at 30 m to 1.13 and 0.88 at 122 m and 396 m, respectively. These differences among the slopes are all statistically significant because in T tests the probabilities for the slopes being the same are 0.011, 0.0034 and 0.0002 between 30 m and 122 m, between 122 m and 396 m and between 30 m and 396 m, respectively. If the boundary layer was truly well mixed and the underlying vegetated surface was homogeneous within the daily footprint, we would expect little variation of the concentration-derived *GPP* with height. The fact that it decreased by about 32% from 30 m to 395 m suggests that either or both conditions were not entirely met. The mixing strength in the PBL depends on the surface heat flux. On clear days, the PBL is generally well mixed, but on cloudy and overcast days, not only the mixing height is lower but the mixing

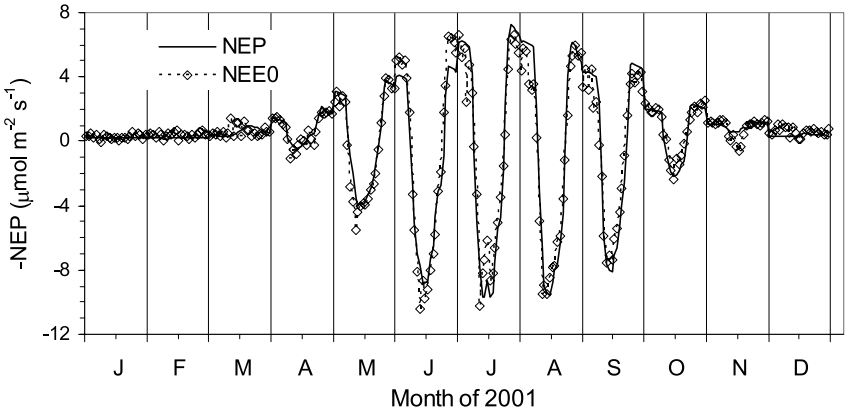

Figure 7. Monthly averages of diurnal variations of modeled $-NEP$ (solid line, upward positive) using an ecosystem model (BEPS) and NEE_0 derived from eddy covariance measurements (symbols) in 2001 at all the three levels and extrapolated to the canopy height.

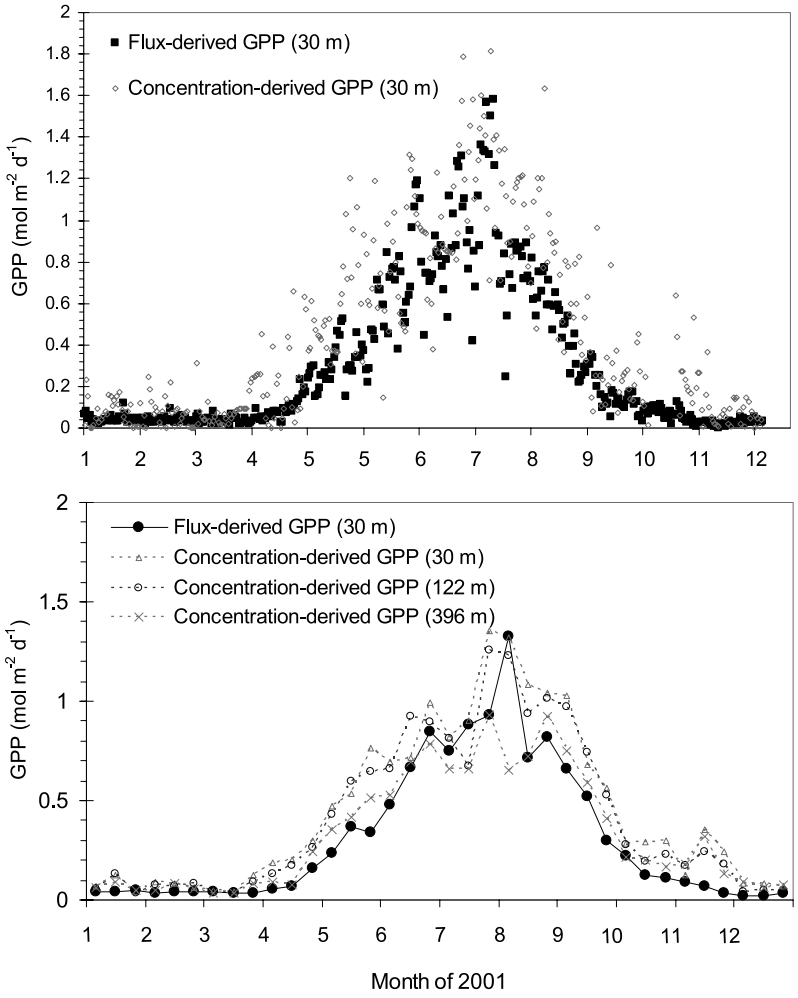

Figure 8. Comparison of concentration-derived daily *GPP* at 30 m, 122 m, and 396 m heights with *GPP* derived from eddy covariance measurements extrapolated to the canopy height in 2001. (top) Daily *GPP*. (bottom) Ten-day averaged *GPP*.

strength at any given height is also weaker, resulting in larger vertical gradients of the measured CO_2. These gradients explain partly the decrease in the concentration-derived *GPP* with height. On clear days, these gradients are small not only within the lower mixed layer as measured at the tower but also throughout the mixed layer as measured by aircraft in Europe [*Karstens et al.*, 2006]. Even on clear days, the mixed layer might have not been entirely well mixed. The Lagrangian timescale for continental mixed layer scaler transport was estimated to range from about 90 s [*Hanna*, 1981] to 15 minutes [*Sorbjan*, 1997], meaning the average time it takes to mix any concentration changes at lower heights to the rest of the boundary layer. Although this timescale is much smaller than the hourly time step, small vertical gradients could not be avoided even on clear days. It is therefore of interest to further investigate this CO_2 vertical gradient under various weather conditions in order to use CO_2 concentration measurements at various heights for upscaling purposes.

[32] The variation of concentration-derived GPP with height could also reflect the heterogeneity of the surface CO_2 flux. As the forest extent is limited (a few tens of km) in all direction around the tower, lakes, croplands, and nonvegetated surfaces at larger distances within the daily footprint (estimated to be a few hundred km) would have larger effects on the concentrations at higher levels. Non-forested areas are expected to have smaller GPP values, and as they are at larger distances from the tower, they therefore can reduce the concentration-derived GPP at higher levels more than lower levels. If we can correct the gradient of CO_2 concentration with height due to inefficient vertical mixing, the concentration-derived GPP at the various heights can be an effective way of estimating the mean fluxes for the landscape of various sizes around the tower.

[33] At 30 m, the concentration-derived *GPP* is larger than the flux-derived *GPP* by about 20% (Figure 9a). This difference cannot be entirely attributed to errors in modeling the vertical mixing because it has been well constrained in modeling the concentration (Figures 4 and 5). The difference could be mostly caused by the fact that the footprint area of the measured CO_2 flux is different from that of CO_2 concentration. CO_2 fluxes measured using eddy covariance techniques depend on the correlation of the fluctuations in CO_2 concentration and the vertical wind speed caused by

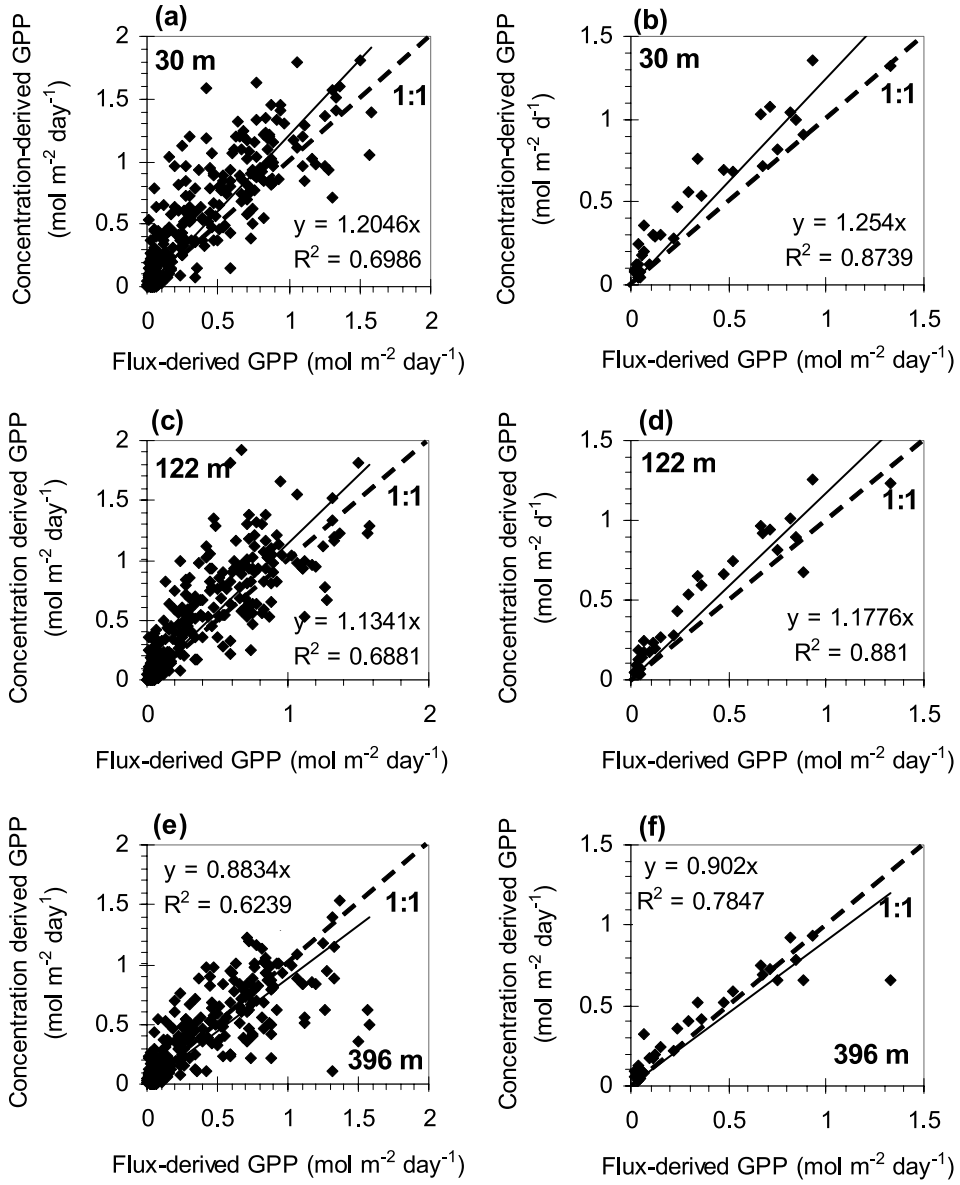

Figure 9. Relationships between concentration-derived daily *GPP* and flux-derived daily *GPP*. (a) Daily values at 30 m. (b) Ten-day averages at 30 m. (c) Daily values at 122 m. (d) Ten-day averages at 122 m. (e) Daily values at 396 m. (f) Ten-day averages at 396 m.

the local surface roughness and the vertical CO_2 gradient, and the typical footprint distance is about 500 m, or a typical footprint area of 1 km^2 [*Schmid*, 2002]. On the other hand, the actual CO_2 concentration contains the accumulated effects of the carbon exchange between the upwind surface and the air parcel. From sunrise to sunset for about 10 hours, the footprint distance is 360 km for an air parcel traveling at a speed of 10 m s^{-1}. The daily footprint area for concentration measurements is therefore estimated to be in the range of 10^3–10^4 km^2, smaller than 10^4–10^5 km^2 for multiple days [*Gloor et al.*, 2001; *Lin et al.*, 2004]. In this study, the concentration-derived GPP may be considered as the regional average of a large footprint area of about 250 km radius from the tower, while the flux-derived *GPP* represent an area within 500 m of the tower. Because the tower is located in the middle of a grassy patch of about 180 m in radius, it is expected that this grassy area had a lower productivity than the surrounding forested area, making flux-derived *GPP* smaller than the concentration-derived *GPP* because of this footprint area difference. Concentration-derived carbon flux information can therefore serve for upscaling from flux towers to the landscape around the tower, which is an intermediate scale and a missing link in the spectrum of spatial scales from sites to the globe.

5. Conclusion

[34] A coupled one-dimensional ecosystem and atmospheric model is used to simulate the CO_2 concentration at various heights within the planetary boundary layer. A

methodology is tested to derive daily GPP values from hourly CO_2 concentration measurements, i.e., to separate the photosynthesis signals from the diurnal CO_2 variation pattern. Separating photosynthesis information from the tower concentration data would add to our ability to upscale from local sites to the landscape and region because the concentration-derived information has a much larger footprint area than tower flux measurements. The following specific conclusions are drawn from this study.

[35] 1. It is possible to derive flux information (e.g., *GPP*) from CO_2 concentration measurements, provided that the associated meteorological measurements are made to allow for modeling the vertical mixing.

[36] 2. Concentration-derived hourly *GPP* decreases with height rapidly in the morning as the nighttime respired CO_2 accumulation at the lower levels is reused by photosynthesis on the subsequent day. However, this height dependence is greatly reduced in the daily *GPP* estimation on the basis of the accumulated effects of surface photosynthesis from sunrise to sunset because in the afternoon and near sunset the boundary layer is well mixed and vertical concentration gradient becomes small. This suggests that daily estimation of *GPP* from concentration may be the most appropriate timescale.

[37] 3. Concentration-derived *GPP* at daily time steps results from a footprint area determined by the travel length and width of the air parcels arriving at the tower over the entire day length from sunrise to sunset. This footprint area is several orders of magnitude larger than an eddy covariance flux footprint which is determined by the efficiency of local vertical mixing. Concentration-derived carbon fluxes can therefore provide information at intermediate scales between local sites and a large region.

[38] **Acknowledgments.** The senior author gratefully acknowledges the financial support of the Canadian Foundation for Climate and Atmospheric Sciences for this research. The major part of this work was conducted during a 3-month sabbatical leave of the senior author at NOAA CMDL, which provided partial financial support. Ken Davis of Pennsylvania State University kindly provided assistance in using the flux data and useful comments on an early draft of this paper.

References

Bakwin, P. S., P. P. Tans, D. F. Hurst, and C. Zhao (1998), Measurements of carbon dioxide on very tall towers: Results of the NOAA/CMDL program, *Tellus, Ser. B*, *50*, 401–415.

Bakwin, P. S., K. J. Davis, C. Yi, S. C. Wofsy, J. W. Munger, L. Haszpra, and Z. Barcza (2004), Regional carbon dioxide fluxes from mixing ratio data, *Tellus, Ser. B*, *56*, 301–311.

Baldocchi, D. D., et al. (2001), Fluxnet: A new tool to study the temporal and spatial variability of ecosystem-scale carbon dioxide, water vapour, and energy flux densities, *Bull. Am. Meteorol. Soc.*, *82*, 2415–2434.

Berger, W. B., K. Davis, and C. Yi (2001), Long-term carbon dioxide fluxes from a very tall tower in a northern forest: Flux measurement methodology, *J. Oceanic Atmos. Technol.*, *18*(2), 529–542.

Burrows, S. N., S. T. Gower, M. K. Clayton, D. S. Mackay, D. E. Ahl, J. M. Norman, and G. Diak (2002), Application of geostatistics to characterize leaf area index (LAI) from flux tower to landscape scales using a cyclic sampling design, *Ecosystems*, *5*(7), 667–679.

Chan, D., C.-W. Yuen, K. Higuchi, A. Shashkov, J. Liu, J. M. Chen, and D. Worthy (2004), On the CO_2 exchange between the atmosphere and the biosphere: The role of synoptic and mesoscale processes, *Tellus, Ser. B*, *56*, 194–212.

Chen, B., J. M. Chen, J. Liu, D. Chan, K. Higuchi, and A. Shashkov (2004), A vertical diffusion scheme to estimate the atmospheric rectifier effect, *J. Geophys. Res.*, *109*, D04306, doi:10.1029/2003JD003925.

Chen, B., J. M. Chen, and D. Worthy (2005), Interannual variability in the atmospheric CO_2 rectification over a boreal forest region, *J. Geophys. Res.*, *110*, D16301, doi:10.1029/2004JD005546.

Chen, J. M., P. M. Rich, T. S. Gower, J. M. Norman, and S. Plummer (1997), Leaf area index of boreal forests: Theory, techniques and measurements, *J. Geophys. Res.*, *102*, 29,429–29,444.

Chen, J. M., J. Liu, J. Cihlar, and M. L. Goulden (1999), Daily canopy photosynthesis model through temporal and spatial scaling for remote sensing applications, *Ecol. Modell.*, *124*, 99–119.

Chen, J. M., W. Ju, J. Cihlar, D. Price, J. Liu, W. Chen, J. Pan, T. A. Black, and A. Barr (2003a), Spatial distribution of carbon sources and sinks in Canada's forests based on remote sensing, *Tellus, Ser. B*, *55*, 622–642.

Chen, J. M., J. Liu, S. G. Leblanc, R. Lacaze, and J.-L. Roujean (2003b), Multi-angular optical remote sensing for assessing vegetation structure and carbon absorption, *Remote Sens. Environ.*, *84*, 516–525.

Chen, J. M., B. Chen, K. Higuchi, J. Liu, D. Chan, D. Worthy, P. Tans, and A. Black (2006), Boreal ecosystems sequestered more carbon in warmer years, *Geophys. Res. Lett.*, *33*, L10803, doi:10.1029/2006GL025919.

Ciais, P., et al. (1997), A three-dimensional synthesis study of $\delta^{18}O$ in atmospheric CO_2: 2. Simulations with the TM2 transport model, *J. Geophys. Res.*, *102*, 5873–5883.

Davis, K. J., P. S. Bakwin, C. Yi, B. W. Berger, C. Zhao, R. Teclaw, and J. Isebrands (2003), The annual cycle of net CO_2 and H_2O exchange over a northern mixed forest as observed from a very tall tower, *Global Change Biol.*, *9*, 1278–1293.

Denning, A. S., I. Y. Fung, and D. Randall (1995), Latitudinal gradient of atmospheric CO_2 due to seasonal exchange with land biota, *Nature*, *376*, 240–243.

Ehleringer, J. R., and C. B. Field (1993), Global constraints and regional processes, in *Scaling Physiological Processes: Leaf to Globe*, pp. 179–190, Elsevier, New York.

Farquhar, G. D., S. von Caemmerer, and J. A. Berry (1980), A biochemical model of photosynthetic CO_2 assimilation in leaves of C3 species, *Planta*, *149*, 78–90.

Fung, I., et al. (1997), Carbon 13 exchanges between the atmosphere and biosphere, *Global Biogeochem. Cycles*, *11*, 507–533.

Gloor, M., P. Bakwin, D. Hurst, L. Lock, R. Draxler, and P. Tans (2001), What is the concentration footprint of a tall tower?, *J. Geophys. Res.*, *106*, 17,831–17,840.

Gurney, K. J., et al. (2002), Towards robust regional estimates of CO_2 sources and sinks using atmospheric transport models, *Nature*, *415*, 626–630.

Hanna, S. R. (1981), Lagrangian and Eulerian time-scale relations in the daytime boundary layer, *J. Appl. Meteorol.*, *20*, 242–249.

Helliker, B. R., J. A. Berry, A. K. Betts, P. S. Bakwin, K. J. Davis, A. S. Denning, J. R. Ehleringer, J. B. Miller, M. P. Butler, and D. M. Ricciuto (2004), Estimates of net CO_2 flux by application of equilibrium boundary layer concepts to CO_2 and water vapor measurements from a tall tower, *J. Geophys. Res.*, *109*, D20106, doi:10.1029/2004JD004532.

Janssens, I. A., et al. (2001), Productivity overshadows temperature in determining soil and ecosystem respiration across European forests, *Global Change Biol.*, *7*, 269–278.

Ju, W., J. M. Chen, T. A. Black, A. Barr, J. Liu, and B. Chen (2006), Modeling coupled water and carbon fluxes in a boreal aspen forest, *Agric. For. Meteorol.*, *140*, 136–151.

Karstens, U., M. Gloor, M. Heimann, and C. Rodenbeck (2006), Insights from simulations with high-resolution transport and process models on sampling of the atmosphere for constraining midlatitude land carbon sinks, *J. Geophys. Res.*, *111*, D12301, doi:10.1029/2005JD006278.

Keeling, C. D., et al. (1989), A three-dimensional model of atmospheric CO_2 transport based on observed winds: 1. Analysis of observational data, in *Aspects of Climate Variability in the Pacific and the Western Americas*, *Geophys. Monogr. Ser.*, vol. 55, edited by D. H. Peterson, pp. 277–303, AGU, Washington, D. C.

Levy, P. E., A. Grelle, A. Lindroth, M. Molder, P. G. Jarvis, B. Kruijt, and J. B. Moncrieff (1999), Regional-scale CO_2 fluxes over central Sweden by a boundary layer budget method, *Agric. For. Meteorol.*, *99*, 169–180.

Lin, J. C., C. Gerbig, S. C. Wofsy, A. E. Andrews, B. C. Daube, C. A. Grainger, B. B. Stephens, P. S. Bakwin, and D. Y. Hollinger (2004), Measuring fluxes of trace gases at regional scales by Lagrangian observations: Application to the CO_2 Budget and Rectification Airborne (COBRA) study, *J. Geophys. Res.*, *109*, D15304, doi:10.1029/2004JD004754.

Liu, J., J. M. Chen, J. Cihlar, and W. Chen (1999), Net primary productivity distribution in BOREAS region from a process model using satellite and surface data, *J. Geophys. Res.*, *104*, 27,735–27,754.

Liu, J., J. M. Chen, J. Cihlar, and W. Chen (2002), Net primary productivity mapped for Canada at 1-km resolution, *Global Ecol. Biogeogr.*, *11*, 115–129.

Mackay, D. S., D. E. Ahl, B. E. Ewers, S. Samanta, S. T. Gower, and S. N. Burrows (2002), Physiological tradeoffs in the parameterization of a model of canopy transpiration, *Adv. Water Res.*, *26*, 179–194.

Mahrt, L., J. Sun, W. Blumen, T. Delany, and S. Oncley (1998), Nocturning boundary-layer regimes, *Boundary Layer Meteorol*, *88*, 255–278.

Moeng, C. H., and J. C. Wyngaard (1989), Evaluation of turbulent transport and dissipation closures in 2nd-order modeling, *J. Atmos. Sci.*, *46*, 2311–2330.

National Oceanic and Atmospheric Administration (2004), GLOBALVIEW-CO_2: Cooperative Atmospheric Data Integration Project—Carbon Dioxide [CD-ROM], Boulder, Colo. [Available on Internet via anonymous FTP to ftp.cmdl.noaa.gov, Path: ccg/co2/GLOBALVIEW]

Newson, M. D., and I. R. Calder (1989), Forests and water resources: Problems of prediction on a regional scale, *Philos. Trans. R. Soc., Ser. B*, *324*, 283–298.

Raupach, M. R. (1995), Vegetation-atmosphere interaction and surface conductance at leaf, canopy and regional scales, *Agric. For. Meteorol.*, *73*, 151–170.

Rodenbeck, C., S. Houweling, M. Gloor, and M. Heimann (2003), CO_2 flux history 1982–2001 inferred from atmospheric data using a global inversion of atmospheric transport, *Atmos. Chem. Phys.*, *3*, 1919–1964.

Schmid, H. P. (2002), Footprint modeling for vegetation atmosphere exchange studies: A review and perspective, *Agric. For. Meteorol.*, *11*, 159–183.

Sorbjan, Z. (1997), Decay of convective turbulence revisited, *Boundary Layer Meteorol.*, *82*, 501–515.

Stull, R. B. (1993), *An Introduction to Boundary Layer Meteorology*, Springer, New York.

Tans, P. P., I. Y. Fung, and T. Takahashi (1990), Observation constraints on the global atmospheric CO_2 budget, *Science*, *247*, 1431–1438.

Valentini, R., et al. (2000), Respiration as the main determinant of carbon balance in European forests, *Nature*, *404*, 861–865.

Wofsy, S. C., and R. C. Harris (2002), The North American Carbon Program (NACP): Report of the NACP Committee of the U. S. Interagency Carbon Cycle Science Program, report, U. S. Global Change Res. Program, Washington, D. C.

Wyngaard, J. C., and R. A. Brost (1984), Top-down and bottom-up diffusion of a scalar in the convective boundary layer, *J. Atmos. Sci.*, *41*, 102–112.

Yi, C., et al. (2000), The influence of advection on measurements of the net ecosystem-atmosphere exchange of CO_2 observed from a very tall tower, *J. Geophys. Res.*, *105*, 9991–9999.

Yi, C., K. J. Davis, B. W. Berger, and P. B. Bakwin (2001), Long-term observations of the dynamics of the continental planetary boundary layer, *J. Atmos. Sci.*, *58*, 1288–1299.

Yi, C., K. J. Davis, P. S. Bakwin, A. S. Denning, N. Zhang, A. Desai, J. C. Lin, and C. Gerbig (2004), Observed covariance between ecosystem carbon exchange and atmospheric boundary layer dynamics at a site in northern Wisconsin, *J. Geophys. Res.*, *109*, D08302, doi:10.1029/2003JD004164.

Zhang, D., and R. Anthes (1982), A high-resolution model of the planetary boundary layer-sensitivity tests and comparisons with SESAME-79 data, *J. Appl. Meteorol.*, *21*, 1594–1608.

B. Chen and J. M. Chen, Department of Geography, University of Toronto, 100 St George St., Room 5047, Toronto, ONT, Canada M5S 3G3. (chenj@geog.utoronto.ca)

P. Tans, Climate Monitoring and Diagnostics Laboratory, NOAA, 325 Broadway, Boulder, CO 80305, USA.